

## ZrOxNy decorative thin films prepared by the reactive gas pulsing process

P. Carvalho<sup>2</sup>, L. Cunha<sup>1</sup>, E. Alves<sup>3</sup>, N. Martin<sup>4</sup>, E. Le Bourhis<sup>5</sup>, F. Vaz<sup>2</sup>

<sup>1</sup>Centro de Física, Universidade do Minho, Campus de Gualtar, 4710-057 Braga, Portugal

<sup>2</sup>Centro de Física, Universidade do Minho, Campus de Azurém, 4800-058 Guimarães, Portugal

<sup>3</sup>Instituto Tecnológico Nuclear, Dept. Física, E.N. 10, 2686-953 Sacavém, Portugal

<sup>4</sup>Institut FEMTO-ST, UMR 6174, CNRS UFC ENSMM UTBM, 26, Chemin de l'épitaphe  
25030 Besancon Cedex, France

<sup>5</sup>Laboratoire de Physique des Matériaux, Université de Poitiers, 86960 Futuroscope, France

### Abstract

Zirconium oxynitride thin films were deposited by dc reactive magnetron sputtering. A zirconium metallic target was sputtered in an Ar + N<sub>2</sub> + O<sub>2</sub> atmosphere. Argon and nitrogen flow rates were maintained constant whereas oxygen was pulsed during the deposition, implementing the reactive gas pulsing process (RGPP). A constant pulsing period  $T = 3$  s was used following an exponential periodic signal versus time. The introduction time of oxygen was systematically changed from 17% to 83% of the period. The RGPP allowed the synthesis of ZrO<sub>x</sub>N<sub>y</sub> films with tuneable metalloid concentrations adjusting the introduction time of the oxygen. Composition and structural variations associated with mechanical, optical and electrical properties exhibited a smooth transition, from metallic-like characteristics, typical of the fcc-ZrN phase, to semi-conducting behaviour corresponding to a mixture of orthorhombic-Zr<sub>3</sub>N<sub>4</sub>(O) and  $\gamma$ -Zr<sub>2</sub>ON<sub>2</sub> crystalline phases.

### 1. Introduction

Reactive magnetron sputtering is a widely used technique to deposit coatings for a wide range of applications, due to the capability of depositing a high range of compound and alloy thin films including oxides, nitrides and carbides [1]. Although reactive sputtering is conceptually simple, it is in fact a complex and non-linear process, which involves many interdependent parameters [2]. A typical feature of the reactive sputtering process is the well-known hysteresis loop of some experimental parameters against the reactive gas (RG) supply in the system [3–7].

For a stable reactive magnetron deposition process, it is advantageous to work with the target surface either fully or partially metallic, while keeping an adequately high partial pressure of the RGs at the substrate, to form the desired compound film. In order to minimize instabilities, several technical improvements have been developed. Some authors proposed to 'overpump' the deposition chamber to eliminate or decrease the hysteresis effect [6, 8, 9]. If the pumping speed

is high enough, the consumption of the RG by the pumping system dominates the consumption of the RG by the growing film. In this case, a gradual transition from the metallic mode to the poisoned mode takes place. This solution is limited due to some technical performances of the pumping units. Another solution has been developed, based on a closed loop control of the RG pressure, or with low frequency pulsing potentials applied to the target [10–13]. The variation of target-to-substrate distance was also experimentally investigated by Schiller *et al* [14]. However, in industry, this variation is not convenient or is usually expensive.

Recent studies mention the use of a non-conventional method to deposit nitride, oxide and oxynitride coatings (which in fact may act for any reactive process), where the RG is introduced in the deposition chamber in a pulsed way: the reactive gas pulsing process (RGPP) [15–19]. The fundamental idea of this method is based on a periodic transition between metal and compound mode, i.e. between the high rate deposition of a metallic-based layer and a subsequent oxidation/nitridation, at high RG partial pressures, corresponding to low deposition rates.

<sup>5</sup> Author to whom any correspondence should be addressed.

In this paper, the RGPP process will be used to deposit decorative zirconium oxynitride thin films. The main focus will be the illustration of the advantages that may come from the use of such an original process, in comparison with the conventional ones, the continuous introduction of the RGs. In a recent study, decorative zirconium oxynitride thin films have been deposited by reactive magnetron sputtering, using a continuous injection of the two RGs ( $N_2$  and  $O_2$ ) [20–23]. It was shown that the composition and structural variations could be divided into different zones, directly related to the deposition conditions. Associated with these compositional and structural zones, a variation in the mechanical, optical and electrical properties was also observed. However, this gas mixture method suffers from plasma instabilities due to the non-linear relationship between the RG flow rate and the sputtering rate of the metallic target, resulting in relatively abrupt transitions between the different compositional and structural zones and thus a consequent abrupt change in the film properties, [20–23]. Thus, the main goal of this work is to explore the possibilities of the RGPP in the attempt to ‘smooth’ the transition of oxynitride thin film properties, and thus explore the wide window of possibilities where these decorative/multifunctional materials might be used. In particular, the smoothening between the different composition zones will have a major effect on the obtained colours, which represents a major point in these decorative-type coatings.

## 2. Experimental details

For this work,  $ZrO_xN_y$  films were deposited on high-speed steel (AISI M2), stainless steel (AISI 316), glass and silicon (100) substrates, by reactive dc magnetron sputtering, in a laboratory-sized deposition system. The films were prepared with the substrate holder positioned 70 mm from the target for all runs, using a dc current density of  $100 \text{ A m}^{-2}$  on the zirconium target (99.96 at% purity). The  $N_2$  gas supply was kept constant ( $q_{N_2} = 10 \text{ sccm}$ ), whereas the oxygen mass flow rate was periodically modulated from  $q_{O_2} = 0$  to  $3 \text{ sccm}$  using an exponential function of time [24]. The cycle period ( $T = t_{ON} + t_{OFF}$ ) was fixed at 3 s. The  $t_{ON}$  time of the oxygen pulse length was systematically changed from 0.5 to 2.5 s, resulting in the variation of the duty cycle  $\alpha = t_{ON}/T$ , from 0.17 to 0.83. The Ar flow was kept constant at  $60 \text{ sccm}$  for all depositions. The working pressure was approximately constant during the depositions (varying slightly between  $\sim 0.4$  and  $0.5 \text{ Pa}$ ). The substrates were grounded and no external heating was used. A delay time of 5 min was used before positioning the surface of the samples in front of the Zr target. This delay time was used to avoid film poisoning resulting from target contaminations from previous depositions and also to assure a practically constant deposition temperature of the substrates during film growth (it was measured to be about  $200 \text{ }^\circ\text{C}$ ).

The atomic composition of the as-deposited samples was measured by Rutherford backscattering spectroscopy (RBS) using (1.4, 1.75) MeV and 2 MeV for the proton and  $^4\text{He}$  beams, respectively. The scattering angles were  $140^\circ$  (standard detector, IBM geometry) and  $180^\circ$  (annular detector), tilt

angles  $0^\circ$  and  $30^\circ$ . Composition profiles for the as-deposited samples were generated using the software code IBA NDF v8.1i<sup>57</sup>. For the  $^{14}\text{N}$ ,  $^{16}\text{O}$  and  $^{28}\text{Si}$  data, the cross-sections given by Ramos *et al* [25] were used. The analysed area was about  $0.5 \times 0.5 \text{ mm}^2$ . In addition, for some samples, proton induced x-ray emission (PIXE) measurements were performed to check for impurities. Ball cratering tests were used to measure the thickness of the samples (used for deposition rate determination).

X-ray diffraction (XRD), using a conventional Philips PW 1710 diffractometer, operating with  $\text{Cu K}\alpha$  radiation, in a Bragg–Brentano configuration, was used to scan the structure and phase distribution of the coatings. Electrical resistivity at room temperature was obtained in the Van der Pauw geometry. Colour coordinates and reflectivity were obtained with a commercial Minolta CM-2600d spectrophotometer (wavelength range: 400–700 nm), using diffused illumination at an  $8^\circ$  viewing angle. The spectrophotometer is equipped with a 52 mm diameter integrating sphere and three pulsed xenon lamps.

Coating hardness was determined from the loading and unloading curves carried out with an ultra-low load depth sensing nanoindenter—Nano Instruments Nanoindenter II, equipped with a Berkovich diamond indenter, operating at a constant displacement rate of  $5 \text{ nm s}^{-1}$ . Hardness values were obtained from the average of 20 measurements at different positions.

## 3. Results and discussion

### 3.1. Evolution of film characteristics: deposition rate and target potential

One of the biggest problems in preparing thin films is related to the poisoning of sputter targets [3, 26–28]. This poisoning results in a significant decrease in the deposition rate (a serious problem in industrial production) as well as an increasing difficulty in having a wide and smooth range of compositions. In previous works, the authors reported the deposition of zirconium oxynitride coatings using a RG mixture composed of nitrogen and oxygen [20, 22]. In these works, it was possible to observe that the deposition rate and target potential evolution could be divided into different modes (regimes), according not only to compositional and structural variations but also in straight correlation with all the film’s properties. Anyway, and although a reasonable set of different samples has been presented, it was clear that, in the transition between the different regimes, as well as within some of these regimes, there were relatively abrupt transitions in the compositional and structural features of the films and, consequently, in the overall film’s properties [20–23].

In order to reduce this drawback, a series of  $ZrO_xN_y$  thin films was prepared, in which oxygen was introduced separately from nitrogen, but in a pulsed manner (the RGPP). A deeper analysis of this type of gas feeding system is described elsewhere [24, 29, 30]. By pulsing the oxygen flow, a constant consumption of this gas is expected. Let us recall that the formation of a zirconium–oxygen bond is energetically more

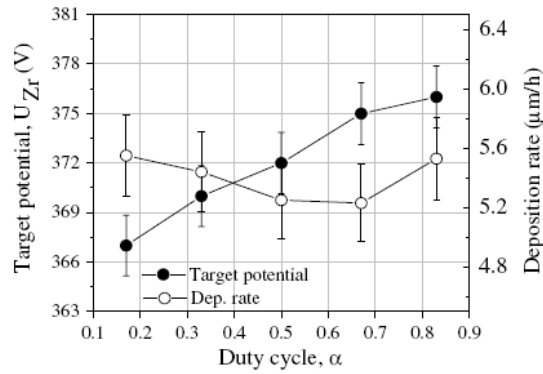


**Figure 1.** Target potential (average values) and deposition rate as a function of the duty cycle. The error bar for the deposition rate values was determined by the maximum deviation to the average value. For the target potential, the error was estimated according to the maximum deviation observed during measurements ( $\sim 2$  V).

favourable ( $\Delta H_f^{\circ} \text{ZrO}_2$ :  $-1042.8 \text{ kJ mol}^{-1}$  [31]) than that of a zirconium–nitrogen bond ( $\Delta H_f^{\circ} \text{ZrN}$ :  $-365.5 \text{ kJ mol}^{-1}$  [32]), reducing in this way the target poisoning, and consequently widening the possibilities of composition and structural changes, and thus the overall film properties. Figure 1 shows the plot of the target potential (average values after stabilization) and deposition rate as a function of the duty cycle,  $\alpha$ .

This plot shows a roughly constant deposition rate of about  $5.4 \mu\text{m h}^{-1}$ , associated with a small increase in target potential from  $\sim 366$  to  $376$  V. This target potential variation is significantly lower than that presented by the samples prepared by the conventional process, CP, which showed an increase with increasing RG flow from 317 to 337 V, within similar compositional values [22] and similar target erosion conditions. This lower level of the increase in the target potential compared with the CP (a sign of a very low degree of target poisoning) should be also responsible of the small variation of the deposition rate (figure 1). This results from the fact that the pulsing of oxygen allows the system to work in equilibrium between the poisoning rate of the target and the cleaning rate, resulting in lower poisoning levels and consequently highest and less varying deposition rates.

### 3.2. Composition and structure evolution of prepared films

The combination of both target potential and deposition rate also has a decisive effect on composition variation, as illustrated in figure 2. The first observation to be noticed is, again, the very smooth evolution of sample's composition, showing an almost constant increase in the oxygen content associated with an also smooth decrease in both nitrogen and zirconium contents. These smooth evolutions contrast with the abrupt transitions observed between the different compositional regions for the zirconium oxynitride coatings, prepared using the CP gas mixture system [21–23]. Moreover, and since these coatings were prepared with the optimized nitrogen flow that was used to deposit stoichiometric ZrN

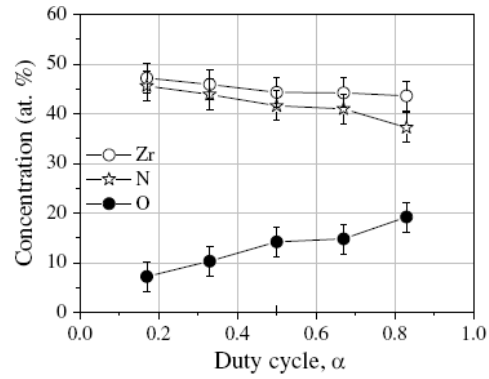


**Figure 2.** Variation of atomic concentrations as a function of the duty cycle. An average of 5 at% was estimated for the RBS concentration resolution.

coatings, no initial increase in all elements was observed in contrast to zirconium oxynitrides films deposited by the RG mixture system, which revealed a very irregular variation in the element's concentration with the increase in gas flow [22, 23]. Regarding the specific values of each element's concentration, the films prepared with duty cycles below 0.5 present an increase in the O content from about 7 ( $\alpha = 0.17$ ) to 14 at% ( $\alpha = 0.5$ ), corresponding to decreases in both Zr and N contents from 47 at% to 44 at% and 46 at% to 42 at%, respectively. This variation tendency suggests that a substitution of N by O may occur, which in fact is consistent with the close stoichiometry condition of the samples ( $(C_N + C_O)/C_{Zr} \sim 1$ ). In these samples, the surface colour tones are roughly golden-yellow with a small increase in redness.

Regarding the samples prepared with duty cycles varying from 0.5 to 0.67, a rough stabilization of all elements' concentration occurs. Finally, the sample prepared with a duty cycle,  $\alpha = 0.83$  exhibits an oxygen content of about 19 at%, which represents a small increase when compared with the one obtained at a duty cycle,  $\alpha$  of 0.67 (15 at%). This last change is associated with a decrease in the N content from 41 ( $\alpha = 0.67$ ) to 37 at% ( $\alpha = 0.83$ ), without any substantial change in the Zr content. Regarding the surface appearances, the samples prepared with  $\alpha \geq 0.5$  present colour tones varying from red-brownish to dark blue, which correlates well with the changes observed within the films from zone II, which were prepared using the CP [21–23]. This means that the same intrinsic colour variation was obtained in this pulsed gas feeding process (RGPP), but avoiding the significant reductions in deposition rates observed in the CP, and allowing a much smoother transition in composition evolutions and thus a correspondingly smoother variation in the films' optical properties (and thus on the overall ones). However, the smooth composition variation of the samples deposited by the RGPP shows that it promotes the formation of richer oxygen samples compared with the CP. The samples deposited by the RGPP system in the interval of non-metal to zirconium ratio from 1.12 to 1.29 present an oxygen content variation of 7 to 20 at%, whereas those deposited with the CP present an oxygen content

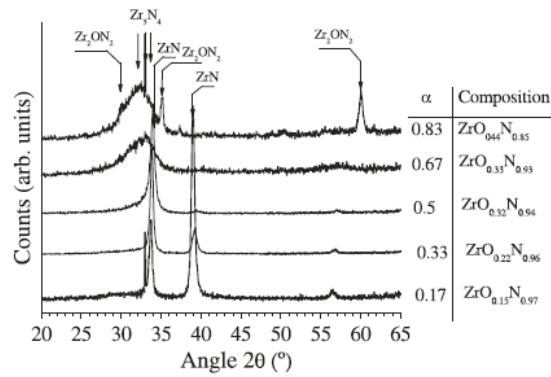


**Figure 3.** XRD patterns for  $ZrO_xN_y$  films as a function of duty cycle.

variation from 5 to 15 at%, with a change in the non-metal to zirconium ratio from 0.9 to 1.4 [23]. Anyway, in the CP, the samples were prepared with a gas mixture composed with a significant excess of N (95%  $N_2$  + 5%  $O_2$  [22] and 85%  $N_2$  + 15%  $O_2$  [23]), which may explain these small oxygen differences. The fact that the same colour evolution was observed induces that the oxygen substitution is probably occurring in the films, where the particular structures that are formed are ruling the overall film's properties.

In order to further uncover these differences in the preparation approaches and to scan the similarities or differences in the structural features occurring in the films, an extensive set of XRD experiments was carried out. Figure 3 shows the XRD patterns of the samples as a function of the duty cycles. The first conclusion that is possible to draw is that the structural evolution is again quite similar to that observed in the samples prepared by the CP [22, 23], revealing a change from a *fcc*-ZrN type structure, to a mixture of both orthorhombic  $Zr_3N_4(O)$  and  $\gamma$ - $Zr_2ON_2$ -type structures, though the appearance of the  $\gamma$ - $Zr_2ON_2$  structure presents some differences in terms of growth planes [22, 23]. Nevertheless, there are few small differences that are worth mentioning. The first and probably the most important one is related to the presence of the *fcc*-ZrN structure in all analyzed coatings, even in the sample with the highest oxygen content ( $\alpha = 0.83$ ), which also presents a mixture of both orthorhombic  $Zr_3N_4(O)$  and  $\gamma$ - $Zr_2ON_2$ -type structures (figure 3). For the samples deposited with CP, the *fcc*-ZrN phase is completely suppressed when the oxynitride phase is present [23], in spite of the lower oxygen content (15 at%). During the  $t_{ON}$  time, the oxygen partial pressure rises and the coatings become more oxygen rich than during the  $t_{OFF}$  time, inducing a lower metal to non-metals ratio. On this basis, it is possible to claim that the RGPP system could promote the preparation of slightly non-homogenous structures, concerning both composition and, consequentially, crystalline structure.

Another difference is related to the formation of the  $\gamma$ - $Zr_2ON_2$ -type structure with lower non-metal to zirconium ratio, in comparison with the sample deposited by the CP. The sample deposited with a duty cycle of 0.83,

where the  $\gamma$ - $Zr_2ON_2$ -type structure is observed, presents a  $C_{Zr}/(C_N + C_O)$  ratio close to 1.29, whereas the samples deposited with the CP requires a non-metal to zirconium ratio close to 1.45 [23]. This difference should be related to the higher oxygen content of the sample deposited by the pulsing process (20 at%), compared with the 15 at% in the gas mixture sample. This ability to deposit coatings with mixed crystalline structures using the pulsing method should be reflected in a smoother properties evolution compared with the CP, which presents a more abrupt transition between the different crystalline structures. The presence of the ZrN-type structure in all the different structural arrangements should have a non-negligible effect, especially in terms of the mechanical and electrical properties evolution.

### 3.3. Optical properties: colour and reflectivity

One of the most important features in oxynitride thin film systems is their optical properties, namely colour. In fact, one of the most promising applications of the zirconium oxynitride system is for decorative purposes. By using the CP, the authors have found a relatively wide window of possible colours, but also some abrupt changes in the film's surface tones, when moving from one compositional zone to the other, and most especially within the first two zones, where only intrinsic-like colours were obtained [22, 23]. Taking this into account, the main goal of this study was to check the influence of the already mentioned smooth composition evolution and more 'mixed' crystalline structures, on the properties of this RGPP series, namely their colour. First of all, it is also important to note that in accordance with structural features, all the prepared films exhibit intrinsic-like colours, corresponding to the same two first zones of the films prepared by the CP [22, 23], but, as mentioned, without that clear two zones films from the CP. Figure 4 shows the evolution of both the film's reflectivity spectra and the corresponding colour coordinates. Comparing the reflectivity spectra of the samples with the evolution of composition (figure 2), it is possible to observe that the progressive increase in oxygen content induces a progressive decrease in reflectivity near the IR region and a shift in the reflectivity minimum to lower energies. Regarding the values of the reflectivity maximum in the red region, there is a clear reduction from 55% for the sample deposited with a duty cycle of 0.17 to about 25% for the sample deposited with the highest duty cycle ( $\alpha = 0.83$ ).

The high values of the reflectivity in the red region are typical of good conductors and are the result of the free-carrier absorption mechanisms. The presence of conduction electrons in high concentration in the materials under study is explained by an overlap between the p- and d-type bands, so that the Fermi level lies inside the d band [33] giving rise to electrical (see next item in this paper) and optical metallic-like behaviour of the films. The significant decrease in the reflectivity maximum red region indicates a clear reduction in the role of the free electrons absorption mechanism in the optical properties of the coatings. Associated with this decrease is the shift to lower energies of the reflectivity minimum. Karlsson *et al* [34] suggested that the observed red shift in the reflectivity minimum can be attributed

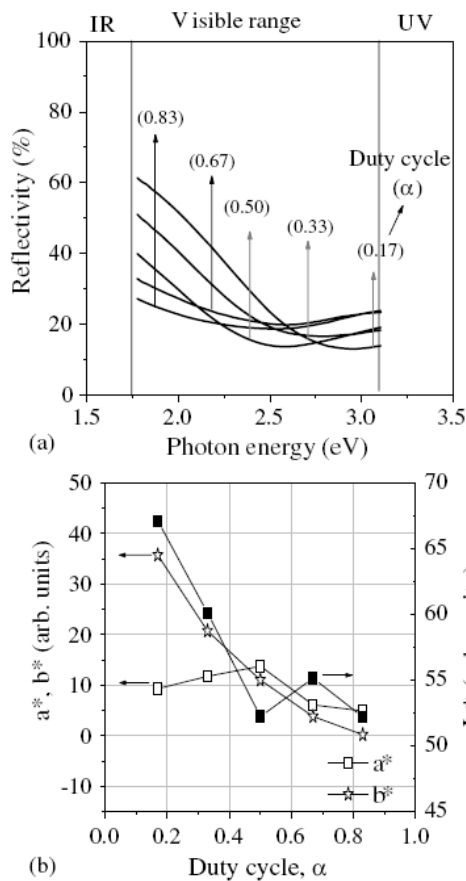


**Figure 4.** (a) Reflectivity spectra as a function of the photon energy and (b) colour coordinates of sputtered  $ZrO_xN_y$  films as a function of duty cycle.

to the decreasing role of conduction electrons in determining the optical properties and, hence, to the less metallic character of the coatings [35].

The  $L^*a^*b^*$  colour space is correlated with the colour evaluation of the human brain, since it indicates colour by accounting the reflectivity spectra and the sensibility of the human eye, in the visible range. The first note that is worth mentioning is the initial decrease in brightness (figure 4(b)), with a good correlation with the compositional variations pointed out above, where a continuous increase in oxygen content associated with a decrease in nitrogen and zirconium content is observed. In order to understand this decrease, one must keep in mind that the brightness of metallic materials is determined by interactions between incident photons and free electrons [36]. Thus, the initial decrease in brightness should be connected to a decrease in the density of states at the Fermi level [37], with the increase in oxygen content due to the increase in the transference of d-electrons from the band at the Fermi level to states between 6 and 9 eV in the O 2p band.

From the chromaticity coordinates evolution (figure 4), it is possible to observe a continuous decrease in  $b^*$  (yellowness)

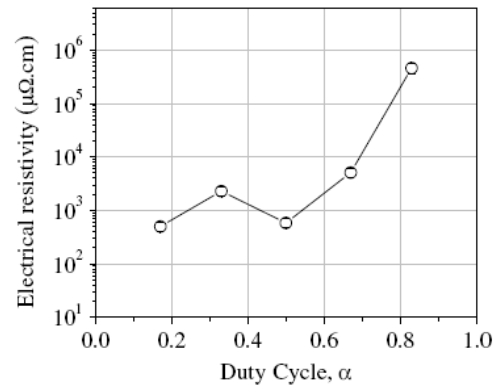


**Figure 5.** Variation of the film electrical resistivity as a function of duty cycle.

associated with a very smooth increase in  $a^*$  followed by an also smooth decrease in this colour coordinate. With the increase in the  $C_O/C_Zr$  ratio, the colour of the coatings changed from golden-yellow to red-brownish and finally dark blue. The colour evolution of the samples deposited with the RGPP is similar to the one obtained with the CP. However, the change occurs in a smoother way (a very important factor at an industrial scale), which allows a better colour control, but also a wider window of different tones, which was clearly one of the most important drawbacks in the preparation of such a decorative film system by the CP. This smoother colour evolution should be related to the gradual compositional changes and thus the mixture of crystalline phases.

#### 3.4. Electrical and mechanical characterization

Figure 5 presents the variation of the dc electrical resistivity at 300 K as a function of the duty cycle. Again, there is a notorious similarity in the electrical resistivity evolution between these coatings and those prepared by the CP, but also with non-negligible differences. The coatings deposited with a duty cycle lower than 0.5 present low values of electrical resistivity, in accordance with the films that actually developed the metallic-like *fcc*-ZrN-type phase. These results are in good accord with those of the same zone of the films prepared by the CP [22, 23].

In previous works the group reported that this oxygen-doped ZrN structure presents a clear non-vanishing of the d band near the Fermi energy with an overlapping between the d and p bands [23]. This non-vanishing DOS at the Fermi energy should explain the metallic conductivity of these coatings [38]. Schwarz *et al* [39] claimed that this overlapping of p and d bands is a sign of metallic-type materials. Moreover, the films prepared with a duty cycle lower than 0.5 presented a small increase in resistivity with increasing temperature (not shown here), which can also be ascribed to the non-vanishing DOS at the Fermi energy.

This first group of films is then followed by a set of others (duty cycles above 0.50) that revealed a progressive increase in resistivity values. It must be remembered that

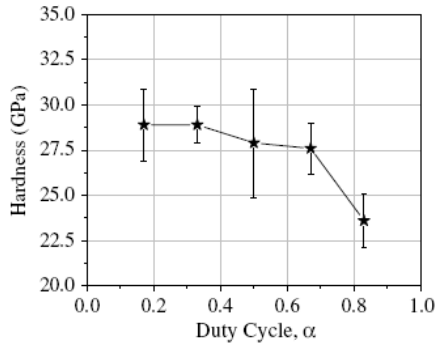


**Figure 6.** Hardness values of sputtered  $ZrO_xN_y$  films as a function of duty cycle.

these coatings presented a progressive formation of *orth*- $Zr_3N_4(O)$  and  $\gamma$ - $Zr_2ON_2$  structures (figure 3). Therefore, the significant increase in resistivity for this set of films should be due to the progressive change in the oxygen-doped ZrN-type structure towards a nitrogen + oxygen-rich phase similar to that of  $Zr_3N_4$ , and also due to the formation of the insulating oxynitride phase, the  $\gamma$ - $Zr_2ON_2$  structure [40], ‘catalyzed’ by the increase in oxygen content. This increase in the oxygen content favours the electronic transfer of zirconium 4d valence electrons to the O 2p regarding the N 2p bands, increasing the ionic character of the bonds and thus the formation of insulator-type material. However, and consistent with the already cited differences in both RGPP and CP series, the electrical resistivity evolution, though revealing low initial resistivity values followed by a strong increase in several orders of magnitude, the RGPP-prepared samples also present some small differences, when compared with the CP-prepared ones. Regarding the samples deposited by the CP, the progressive formation of the *orth*- $Zr_3N_4(O)$  and  $\gamma$ - $Zr_2ON_2$  structures was followed by an increase in the electrical resistivity values from  $1 \times 10^3$  to  $2 \times 10^{15} \mu\Omega \text{ cm}$ , whereas for the RGPP case, this increase is only from  $1 \times 10^3$  to  $9 \times 10^5 \mu\Omega \text{ cm}$ , despite the higher oxygen content in the RGPP samples. This lower variation should result from the already referred mixture of crystalline phases. It must be remembered that the RGPP samples that developed the *orth*- $Zr_3N_4(O)$  and  $\gamma$ - $Zr_2ON_2$  structures ( $\alpha = 0.83$ ) are still presenting some traces of the *fcc*-ZrN structure. Since both  $Zr_3N_4$  and  $Zr_2ON_2$  are known to be of the insulating type (even more if we take into account the most probable doping of the first one by oxygen), a higher increase in electrical resistivity values should be expected. However, the presence of the ZrN phase, known as a conductive material, should be responsible for the lower electrical resistivity increase.

The influence of the duty cycle variation and its effect on the composition and structural features of the films can also be correlated with the evolution of the mechanical properties, as illustrated in figure 6. All the coatings present loading and unloading curves that are approximately parabolic (not shown here). This is a good indication of a significant accommodation of elastic deformation. Figure 6 shows that the evolution of

coatings hardness is characterized by a small decrease in this parameter for the coatings deposited with duty cycle lower than 0.67, followed by an abrupt decrease in this film property, reaching a value of about 23 GPa for the sample prepared with the highest duty cycle ( $\alpha = 0.83$ ).

The decrease in hardness values, especially for the last sample ( $\alpha = 0.83$ ), should result from the decrease in the covalent bonding character of the coatings [41]. Covalent nitrides such as ZrN are more attractive candidates for achieving high hardness than ionic compounds (such as  $\gamma$ - $Zr_2ON_2$ ) since electrostatic interactions are omnidirectional and yield low bond-bending force constants, which result in low shear modulus.

Similar to the other properties, the hardness evolution of the samples deposited by the RGPP process presents a much smoother variation with the increase in oxygen content, as compared with the samples deposited by CP. In previous works, the authors reported that zirconium oxynitride coatings deposited by the CP present a similar trend as reported here for the RGPP samples [22]. However, this decrease was much more pronounced, varying from 35 to 25 GPa. Once again, the smoother compositional and structural changes should be responsible for the decrease in the smooth hardness values. Nevertheless, the samples deposited by CP present higher hardness values compared with the RGPP samples within the similar composition range. Anyway, the primordial application of these coatings is for decorative purposes, this difference should not be a drawback since the coatings present hardness values similar to those of zirconium nitride [42, 43], which is commonly used as a decorative coating.

#### 4. Conclusion

The reactive sputter deposition of zirconium oxynitride thin films was successfully implemented with the RGPP. Argon and nitrogen gases were continuously supplied into the sputtering chamber whereas the oxygen mass flow rate was pulsed versus time using an exponential signal. A constant pulsing period  $T = t_{ON} + t_{OFF}$  was used whereas the  $t_{ON}$  time of the oxygen pulse length was changed from 0.5 to 2.5 s (duty cycle  $\alpha = t_{ON}/T$  from 17% to 83% of  $T$ ).

Small variations of the deposition rate associated with small changes in the target potential versus duty cycle allowed the Zr–O<sub>2</sub>–N<sub>2</sub> system to work in alternation between oxidized and nitrided sputtering modes. Similarly, a very smooth evolution of the  $ZrO_xN_y$  film composition as a function of the duty cycle was produced. In contrast to the CP no distinct regions could be observed. Films prepared with duty cycles lower than 0.5 exhibited a *fcc*-ZrN type structure suggesting a substitution of N atoms by O ones. For higher duty cycles, a mixture of both orthorhombic  $Zr_3N_4(O)$  and  $\gamma$ - $Zr_2ON_2$  phases were mainly prepared. Colour tones also showed some gradual changes for the same range of duty cycles. Surface colours were roughly golden-yellow with a slight redness in the first region. Red-brownish to dark blue colours were obtained in the second one.

The metallic-type behaviour (attributed to an overlapping of the d and p bands) was also observed from resistivity

measurements of  $ZrO_xN_y$  films deposited in the first region ( $\alpha < 0.5$ ). The highest resistivities were correlated with the occurrence of a phase mixture (*orth*- $Zr_3N_4$  (O) and  $\gamma$ - $Zr_2ON_2$ ) and the increased oxygen concentration. Both favour the ionic character of the bonds and the deposited compound tends to behave as an insulator.

Finally, gas pulsing prevented significant reductions in deposition rates peculiar to the CPs, and also led to a much smoother and well-controlled transition of compositions, structure and multi-functional behaviour of zirconium oxynitride thin films.

## Acknowledgment

The authors thank the 'Fundação para a Ciência e Tecnologia' of Portugal for the project PTDC/CTM/69362/2006.

## References

- [1] Graham M E and Sproul W D 1994 *Proc. SVC 37th Annual Technical Conf. (Boston, MA, 8–13 May 1994)* p 275
- [2] Tsiogas C D and Avaritsiotis J N 1992 *J. Appl. Phys.* **71** 5173
- [3] Kinbara A, Kusano E and Baba S 1992 *J. Vac. Sci. Technol. A* **10** 1483
- [4] Hohnke D K, Schmatz D J and Hurley M D 1984 *Thin Solid Films* **118** 301
- [5] Westwood W D, Maniv S and Scanlon P J 1983 *J. Appl. Phys.* **54** 6841
- [6] Berg S, Blom H O, Larsson T and Nender C 1987 *J. Vac. Sci. Technol. A* **5** 202
- [7] Affinito J and Parsons R R 1984 *J. Vac. Sci. Technol. A* **2** 1275
- [8] Okamoto A and Serikawa T 1986 *Thin Solid Films* **137** 143
- [9] Spencer A G, Howson R P and Lewin R W 1988 *Thin Solid Films* **158** 141
- [10] Sproul W D, Christie D J and Carter D C 2005 *Thin Solid Films* **491** 1
- [11] Este G and Westwood W D 1984 *J. Vac. Sci. Technol. A* **00202** 1238
- [12] Hmiel A F 1985 *J. Vac. Sci. Technol. A* **3** 592
- [13] Billard A, Mercs D, Perry F and Frantz C 2001 *Surf. Coat. Technol.* **140** 225
- [14] Schiller S, Beister G and Sieber W 1984 *Thin Solid Films* **111** 259
- [15] Aronson A J, Chen D and Class W H 1980 *Thin Solid Films* **72** 535
- [16] *US Patents* 4,428,811 and 4,428,812
- [17] Howson R P, Danson N and Safi I 1999 *Thin Solid Films* **351** 32
- [18] Martin N, Lintymer J, Gavaille J and Takadoum J 2002 *J. Mater. Sci.* **37** 4327
- [19] Sproul W D 1987 *Surf. Coat. Technol.* **33** 73
- [20] Vaz F, Carvalho P, Cunha L, Rebouta L, Moura C, Alves E, Ramos A R, Cavaleiro A, Goudeau Ph and Rivière J P 2004 *Thin Solid Films* **469–470** 11
- [21] Carvalho P, Vaz F, Rebouta L, Carvalho S, Cunha L, Goudeau Ph, Rivière J P, Alves E and Cavaleiro A 2005 *Surf. Coat. Technol.* **200** 748
- [22] Carvalho P *et al* 2005 *J. Appl. Phys.* **98** 023715
- [23] Carvalho P, Chappé J M, Cunha L, Lanceros-Méndez S, Alpuim P, Vaz F, Alves E, Rousselot C, Espinós J P and González-Elipé A R 2008 *J. Appl. Phys.* **103** 104907
- [24] Martin N, Lintymer J, Gavaille J, Chappé J M, Sthal F, Takadoum J, Vaz F and Rebouta L 2007 *Surf. Coat. Technol.* **201** 7720
- [25] Ramos A R, Paúl A, Rijniens L, Da Silva M F and Soares J C 2002 *Nucl. Instrum. Methods B* **190** 95
- [26] Sproul W D, Graham M E, Rudnik P J and Wong M S 1997 *Surf. Coat. Technol.* **89** 10
- [27] Schiller H, Heisig U, Beister G, Steinfeld K, Strumpfel J, Korndorfer C and Sieber W 1984 *Thin Solid Films* **118** 255
- [28] Safi I 2000 *Surf. Coat. Technol.* **127** 203
- [29] Martin N, Lintymer J, Gavaille J, Chappé J M, Sthal F, Takadoum J, Vaz F and Rebouta L 2007 *Surf. Coat. Technol.* **201** 7727
- [30] Martin N, Lintymer J, Gavaille J, Chappé J M, Sthal F, Takadoum J, Vaz F and Rebouta L 2007 *Surf. Coat. Technol.* **201** 7733
- [31] Lide D R (ed) 2003–2004 *Handbook of Chemistry and Physics* 84th edn (Boca Raton, FL: CRC Press) pp 5–23
- [32] Ma X, Li C, Bai K, Wu P and Zhang W 2004 *J. Alloys Compounds* **373** 194
- [33] Delin A, Eriksson O, Ahuja R, Johansson B, Brooks M S S, Gasche T, Auluck S and Wills J M 1996 *Phys. Rev. B* **54** 1673
- [34] Karlsson B, Shimshock R P, Seraphin B O and Haygarth J C 1983 *Sol. Energy Mater.* **7** 401
- [35] Veszeilei M, Andersson K, Ribbing C G, Järrendahl K and Arwin H 1994 *Appl. Opt.* **33** 1993
- [36] Ohring M 1992 *The Materials Science of Thin Films* (San Diego, CA: Academic)
- [37] Pierson J F, Bertran F, Bauer J P and Jolly J 2001 *Surf. Coat. Technol.* **142–144** 906
- [38] Milošev I, Strehblow H H and Navinsek B 1997 *Thin Solid Films* **203** 246
- [39] Schwarz K, Ripplinger H and Neckel A 1982 *Z. Phys. B* **48** 79
- [40] Bazhanov D I, Knizhnik A A, Safonov A A, Bagatur'yants A A, Stoker M W and Korkin A A 2005 *J. Appl. Phys.* **97** 044108
- [41] Haines J, Léger J M and Bocquillon G 2001 *Annu. Rev. Mater. Res.* **31** 1
- [42] Auger M A, Araiza J J, Falcony C, Sánchez O and Albella J M 2007 *Vacuum* **81** 1462
- [43] Mitsuo A, Mori T, Setsuhara Y, Miyake S and Aizawa T 2003 *Nucl. Instrum. Methods B* **206** 366